#6176

NUMERICAL PREDICTION OF FLOWS CONFINED BY IRREGULAR BOUNDARIES, OF RELEVANCE TO ROOM VENTILATION

F. A. Castro and A. Restivo
Faculty of Engineering. University of Porto
Porto, Portugal

SUMMARY

The paper examines the performance of a numerical procedure suitable to handle flows confined by irregular boundaries, when applied to room ventilation. The calculations presented employ a two-dimensional procedure for solving time-averaged equations on a co-located non-orthogonal grid fitted to the boundaries of the flow domain. The algebraic equations are obtained by integration over finite volumes and solved iteratively with the SIMPLE algorithm. Turbulent transport is approximated through the K-ε model, in a version suitable to handle low Reynolds number flows, as occur near solid boundaries.

The results concentrate on simple geometries. Firstly, a rectangular enclosure with full span inlet and outlet openings, for which calculated results have been published, is again investigated. It is shown that the present calculations are in reasonable agreement with previous predictions obtained with turbulent wall functions.

Then, flows in non-orthogonal geometries are considered, to take full advantage of the flexibility of the present procedure. The results demonstrate that it is now possible, within reasonable limits of computer resources and cost, to calculate practical flows encountered in ventilated rooms.

INTRODUCTION

The report examines the numerical prediction of flows in ventilated rooms with non-rectangular boundaries. Numerical procedures, based on finite difference formulations, have been in use for several years and allow the calculation of ventilation flows in simple geometries, typically rectangular enclosures. The inherent limitations of such procedures virtually precluded the computational study of more realistic flows, such as occur in occupied spaces, or rooms with irregular boundaries.

However, recent developments in numerical methods brought increased flexibility to the application of finite difference based procedures, namely through the use of non-orthogonal grids, providing the capabilities needed to handle complex flow boundaries.

The reported work will attempt to evaluate the performance of a procedure of the latter type, which is a development of a two-dimensional implementation of the SIMPLE algorithm, derived from a code originally employing staggered grids for the components of velocity, as described for example in reference [1]. In order to cope with non-orthogonal coordinates, the code was firstly adapted to employ the same grid for all calculated variables. Secondly, the physical domain was mapped into a rectangular domain in computational space, in such a way that the physical boundaries become the sides of the computational rectangle, and the momentum and continuity equations were cast in a form that reflects the coordinate transformation. And finally, the transformed equations were solved numerically, with the SIMPLE algorithm.

Turbulent transport was modelled with the K-ε model, but the near wall regions were also discretized and calculated directly, avoiding the more common practice of prescribing the flow through standard wall functions. The calculation of the low turbulence near wall layers required a low Reynolds number formulation of the K-ε model.

The various areas of development resulted in a code that is expected to perform better, in many respects, than the original procedure from which it derived, but a quantitative assessment was necessary, and the paper provides the main results of it.

Preliminary tests were performed with a rectangular geometry previously studied by one of the authors [2], both experimentally and numerically. The purpose of the tests has been to check the validity of the low Reynolds number near wall calculations and provide evidence of the grid refinement needed to adequately represent the main features of the mean flow.

The procedure was subsequently employed to calculate the flow in a ventilated room with an inclined section in its ceiling and in a room with a sloping floor, typical of a conference hall. The results presented are mainly intended to demonstrate that a wide variety of geometries are now within the limits of procedures of the present type.

The following section describes the numerical procedure, and the calculated results are subsequently presented in detail. The report closes with a discussion of the main findings of the calculations and summary conclusions.

NUMERICAL PROCEDURE

The procedure employed to obtain the reported results is based upon the SIMPLE algorithm. The momentum equations are solved directly, using the components of velocity as main variables, and the pressure is obtained iteratively through a pressure correction

equation, that in each iteration is derived by enforcing mass conservation to the computed velocity distribution.

The turbulent Reynolds stresses are modelled through a turbulent viscosity, which in turn is expressed in terms of the distributions of the turbulent kinetic energy K and its dissipation rate ε. These turbulence quantities are calculated from adequate transport equations and, together with the expression for the turbulent viscosity, form the well known K-ε model. With all equations written in conservative form, a common format may be adopted. Representing by the general variable ϕ any of the dependent quantities involved, the equations to be solved are of the type

$$\frac{\partial}{\partial x^j}(\rho u_k \phi) = \frac{\partial}{\partial x^j}\left(\Gamma_\phi \frac{\partial \phi}{\partial x^m}\right) + S_\phi \qquad (1)$$

Table 1 lists the diffusivities and source terms used in each case.

ϕ	Γ_ϕ	S_ϕ
1	0	0
u_i	$\mu+\mu_t$	$\frac{\partial}{\partial x^j}\left((\mu+\mu_t)\frac{\partial u_k}{\partial x_m} - p\right) + S_{u_i}$
k	$\frac{\mu_t}{\sigma_k}+\mu$	$(G-\rho\varepsilon)$
ε	$\frac{\mu_t}{\sigma_\varepsilon}+\mu$	$\left(c_1 f_1 \frac{\varepsilon}{k} G - c_2 f_2 \rho \frac{\varepsilon^2}{k}\right)$

Table 1. Diffusivities and source terms in transport equations to be solved.

The turbulent viscosity is calculated as follows:

$$\mu_t = c_\mu f_\mu \rho \frac{k^2}{\varepsilon} \qquad (2)$$

The constants in the K and ε equations have the accepted values:

$$\sigma_\varepsilon = 1.22,\ \sigma_\varepsilon = 1.0,\ C_1 = 1.44,\ C_2 = 1.92,\ C_\mu = 0.09$$

The above modelled forms are suitable for high turbulence Reynolds numbers, and are also described, for example, in reference [2].

To solve the equations numerically, they were first cast into algebraic relations representing the same conservation principles in finite volumes, that result from a subdivision of the physical domain. Earlier codes limited this partition to volumes with simple geometry, namely volumes with faces that are coordinate surfaces of carthesian or cylindrical coordinate systems. As a result, only elementary geometries could be tackled efficiently.

In order to overcome this limitation, the procedure employed here handles general coordinate systems. The only requirement is that the boundaries of the physical domain be

coordinate surfaces (coordinate lines in two dimensions), in order to allow easy manipulation of boundary conditions and enable the use of a structured grid, which has many advantages in terms of computational economy. Detailed analyses of the problems involved in generating coordinate systems for arbitrary flow domains may be found, for example, in references [3] and [4].

In two dimensions, we assume that a suitable coordinate system has been devised, such that the physical domain, in the (x_1,x_2) plane, is maped into a rectangle in the computational plane (ξ_1,ξ_2), see figure 1.

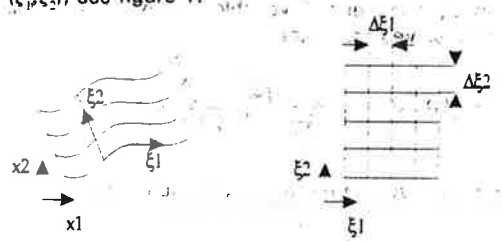

Figure 1. Physical and computational domains.

The transformation of coordinates is represented by the equations:

$$x^1 = X(\xi^1,\xi^2), \quad x^2 = Y(\xi^1,\xi^2) \tag{3}$$

Introducing the Jacobian matrix of the transformation and its determinant J, the spatial derivatives in the physical plane are also transformed into the computational plane:

$$Dx(\xi) = \begin{bmatrix} \frac{\partial x^1}{\partial \xi^1} & \frac{\partial x^1}{\partial \xi^2} \\ \frac{\partial x^2}{\partial \xi^1} & \frac{\partial x^2}{\partial \xi^2} \end{bmatrix}, \quad \beta_k^j = J\frac{\partial \xi^j}{\partial x^k} \tag{3.1}$$

The transport equations to be solved may then be written in terms of the computational coordinates (ξ_1,ξ_2). After some manipulation, the transformed equations for momentum and mass conservation may be arranged as follows:

$$\frac{1}{J}\frac{\partial}{\partial \xi^j}(\rho u_k \beta_k^j) = 0 \tag{4}$$

$$\frac{\partial}{\partial \xi^j}(\rho u_k \beta_k^j u_i) = \frac{\partial}{\partial \xi^j}\left[\frac{\mu_t+\mu}{J}\left(\frac{\partial u_i}{\partial \xi^m}\beta_k^m\beta_k^j + \frac{\partial u_k}{\partial \xi^m}\beta_i^m\beta_k^j\right)\right] - \frac{\partial}{\partial \xi^j}(p\beta_i^j) + S_{u_i} \tag{5}$$

The primitive velocity components, together with pressure, remain the dependent variables to be calculated numerically.

The above equations are integrated in the computational domain, which is rectangular in shape and lends itself easily to a scheme similar to the conventional implementations of SIMPLE in carthesian coordinates.

However, both velocity components are now required in all volume faces, in order to compute the mass fluxes, and so the staggered grid arrangement, commonly adopted in such implementations, would entail the need for additional interpolations. Instead, the

present procedure makes use of a single grid, where all velocity components, pressure and any additinal scalar quantities are calculated.

This non-staggered approach has been explored in previous works [5, 6] and shown to lead to an efficient procedure, provided that the velocity components at the volume faces are represented by a pressure-weighted interpolation that prevents the oscillatory pressure distributions encountered in previous studies.

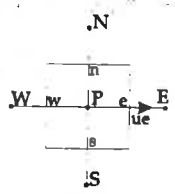

Figure 2. Location of nodes and interfaces in finite volume.

With reference to figure 2, the U-component of velocity at the volume interface between nodes P and E, designated Ue, is obtained by averaging the coefficients of the algebraic equations for U at these two nodes, in the following way:

$$(u_{ie}^{*})^{n} = \alpha_{u_i}\left(\frac{\sum_j a_j (u_i^{*})_j + b' - (p_n^{*}-p_s^{*})\beta_i^2}{a_p}\right)_e - \alpha_{u_i}\left(\frac{\beta_i^1}{a_p}\right)_e (p_E^{*}-p_P^{*}) + (1-\alpha_{u_i})(u_{ie}^{*})^{n-1} \qquad (6)$$

However, the pressure gradient term introduces the pressures at adjacent nodes, and so oscillations in pressure are effectively filtered mass conservation is enforced by the pressure correction equation. The present procedure also took into consideration the findings of reference [7], in order to make the interpolated fluxes consistent with the relaxation factors used in solving the algebraic equations.

The transport equations for K and ε were also transformed in a similar manner. In addition, the turbulence model was written in a form suitable to compute the flow in the vicinity of solid boundaries. The modifications introduced account for low turbulence Reynolds numbers and for the damping effect of the solid walls, expressed in terms of non-dimensional quantities R_t and R_y, respectively. The corresponding effects are represented by correction factors applied to the constants C_μ, C_1 and C_2, given by:

$$f_\mu = [1-\exp(-0.0165R_y)]^2 \times (1+\frac{20.5}{R_t})$$

$$f_1 = 1+(\frac{0.05}{f_\mu})^3 \quad , \quad f_2 = 1-\exp(-R_t^2)$$

$$R_t = \rho\frac{k^2}{\mu\varepsilon} \quad , \quad R_y = \rho\sqrt{k}\frac{Y}{\mu}$$

The low Reynolds number formulation of the K-ε model is described in [8] and the correction factors adopted here were proposed in [9].

The complete set of equations has been solved iteratively, using a line by line TDMA solver. Boundary conditions at solid surfaces were, for all reported calculations, null values for the boundary velocity components, turbulent kinetic energy and dissipation.

CALCULATED RESULTS

The geometries studied here are sketched in figure 3, together with the relevant scales that identify them.

The calculations to be presented were all performed in a VAX 6520 computer. Converged solutions required approximately 350 min CPU time with the finest grids employed.

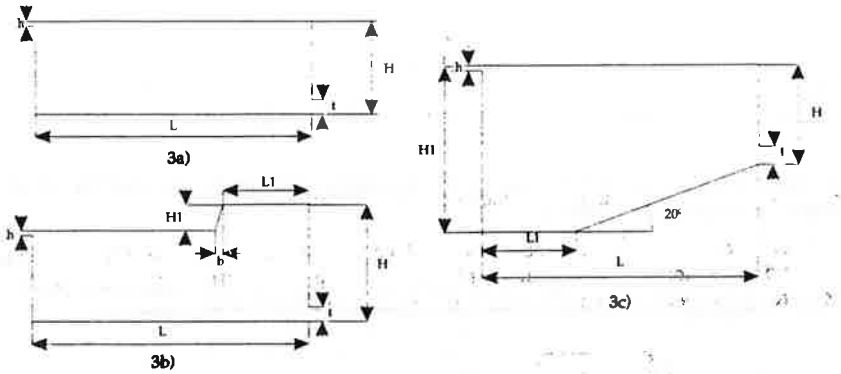

Fig.3. Geometries of the present study.

Preliminary tests were conducted with a geometry already adopted in reference [2]. It represents a rectangular enclosure with full width inlet and outlet slots, as shown in figure 3 a. The geometrical parameters are $h/H=0.056$, $L/H=3$ and $t/h=0.16$.

The tests aimed to check the calculated results against previous predictions performed with a two-dimensional version of the TEACH computer programme. Since the geometry is rectangular, any differences between the two results may be directly attributed to the use of turbulent wall functions in [2], compared to the direct calculation of the near wall regions in the present case.

The calculations reported here were carried out for two Reynolds numbers, 5000 and 10000 (based on inlet conditions), and for meshes of 50x50 and 101x101 grid nodes. The inlet boundary conditions, as in all subsequent calculations, were uniform velocity, turbulence kinetic energy corresponding to 5% turbulence intensity and dissipation corresponding to a length scale equal to the inlet height h. Results are presented in figures 4a, 4b and 4c, in terms of streamline patterns (stream function is normalized with the inlet volume flow rate). Figures 5a and 5b depict vertical profiles of longitudinal velocity, turbulence kinetic energy, energy dissipation and effective viscosity.

These results were obtained with non-uniform grids, as a substancial concentration of grid lines was required to ensure that the first line adjacent to a solid boundary lies within the viscous sublayer, and the steep gradients of the turbulence variables are apropriately reproduced.

Special care was exerted to obtain stable distributions of all variables near the boundaries, where K and ε approach zero and, due to the way in which they are combined in equation 2, tend to induce large fluctuations of turbulent viscosity from iteration to iteration in the near wall region. It was found that the adoption of a large initial value of turbulent viscosity in all nodes, of at least 100 times the fluid viscosity, and strong under-relaxation in updating the turbulent viscosity, were sufficient to eliminate the observed difficulties.

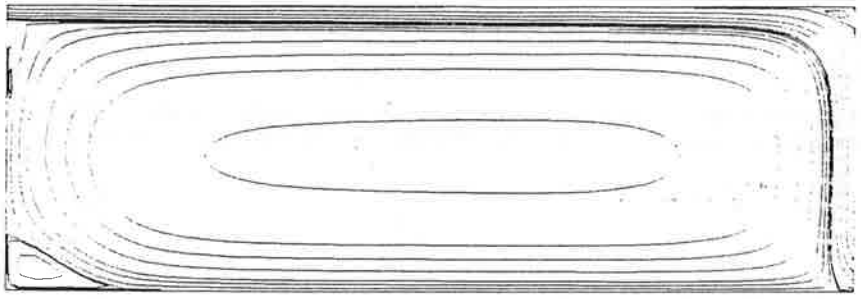

Fig. 4a. Streamline pattern for the flow in the geometry of figure 3a. Re = 5000, 101x101 grid nodes. Ψ/(h.Uin) in the interval [1.03, -2]

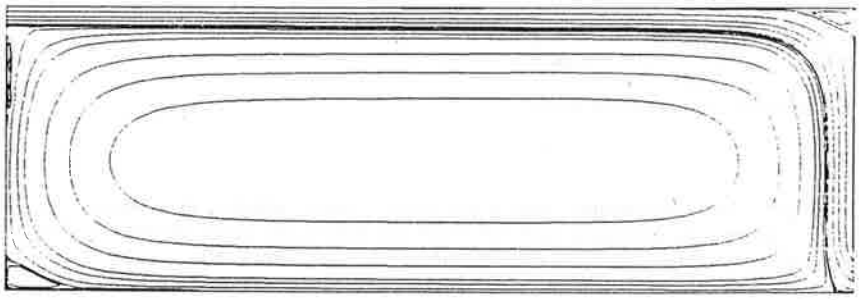

Fig. 4b. Streamline pattern for the flow in the geometry of figure 3a. Re = 10000, 101x101 grid nodes. Ψ/(h.Uin) in the interval [1.03, -1.33]

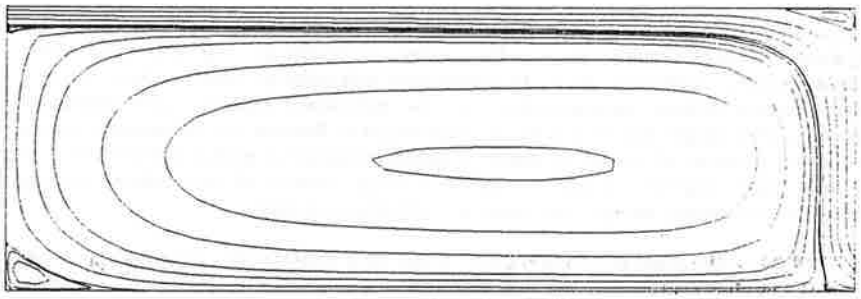

Fig. 4c. Streamline pattern for the flow in the geometry of figure 3a. Re = 10000, 50x50 grid nodes. Ψ/(h.Uin) in the interval [1.03, -1.33]

The vertical profile of longitudinal velocity, computed at x/H = 2 with the same conditions as in figure 5, is shown in figure 6, and the calculated results from [2] are superimposed, to enable an assessment of the relative differences that may be attributed to the different representations of the near wall flow.

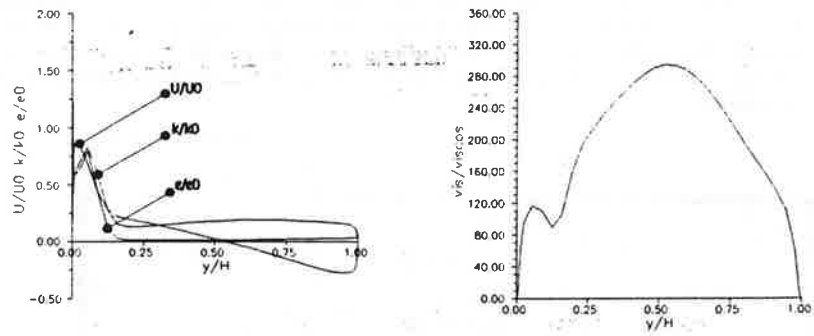

Fig.5a. Calculated profiles of U, K, ε and μ_t/μ at x/H=1. Re=10000. 50x50 grid nodes.

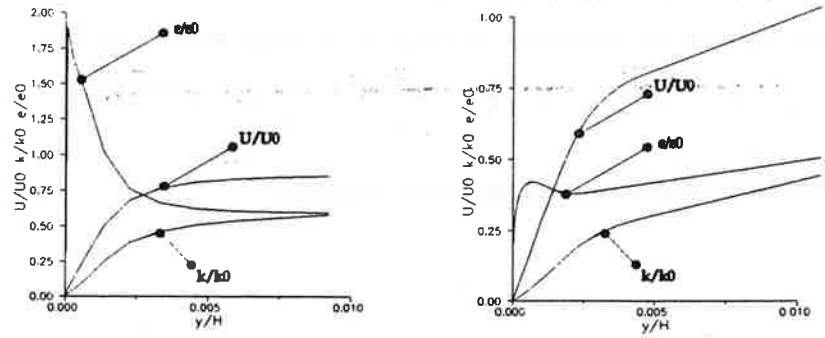

Fig.5b. Detailed profiles of U, K and, ε at x/H=1, near the ceiling. Re=10000. 50x50 and 101x101 grid nodes.

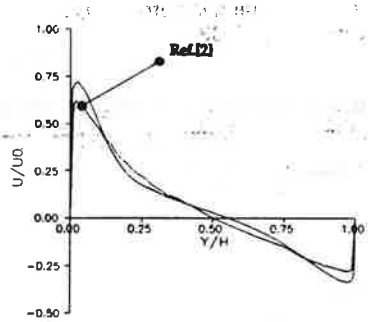

Fig.6. Calculated profiles of U at x/H=2. Present calculations (Re=10000. 50x50 grid nodes) and results from reference [2].

The present procedure was then applied to predict the ventilation flow in geometries with non-rectangular boundaries. One is a room with a partially elevated ceiling, as sketched in figure 3b. The relevant scales are h/H=0.056, L/H=3 and t/H=0.16, as in the previous case, and L1/H=1, H/H1=3.5 , b/H1=0.33

The grid employed, again with 50x50 nodes, is shown in figure 7. For simplicity, it has been derived from a carthesian grid by uniformly expanding the vertical size to fit the

contour of the ceiling. The Reynolds number has been fixed at 10000. The calculated streamline pattern is shown in figures 8 and 9, the latter being a close-up view of the zone that contains the elevated section. This tes was particularly severe for the procedure, due to the skewness of the grid lines near the inclined boundary, which tends to deteriorate the rate of convergence.

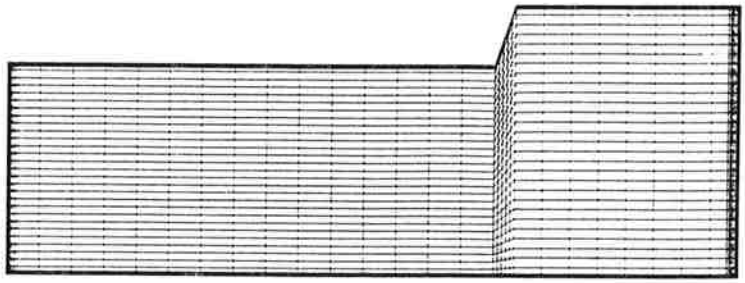

Fig.7. Grid adopted to calculate the flow in a geometry of the type shown in fig. 3.b.

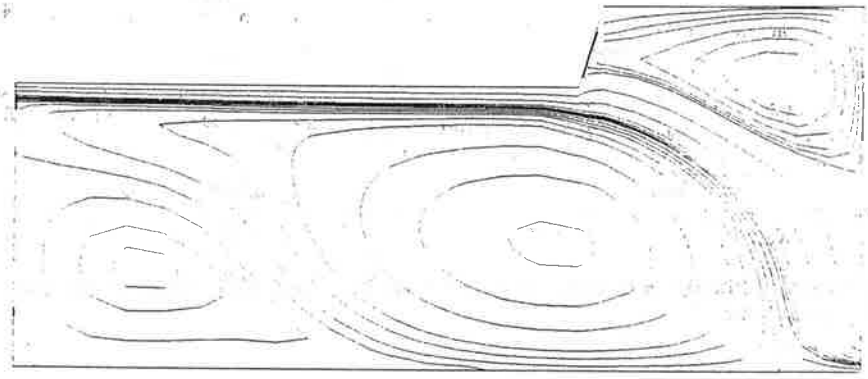

Fig.8. Streamline pattern of the flow in a geometry of the type shown in fig. 3.b. $\Psi/(h.Uin)$ in the interval [1.3,-1.3]

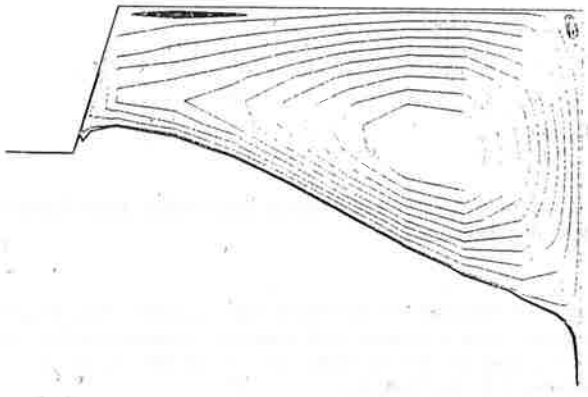

Fig.9. Close-up view of figure 8. Flow beneath the inclined ceiling and elevated section.

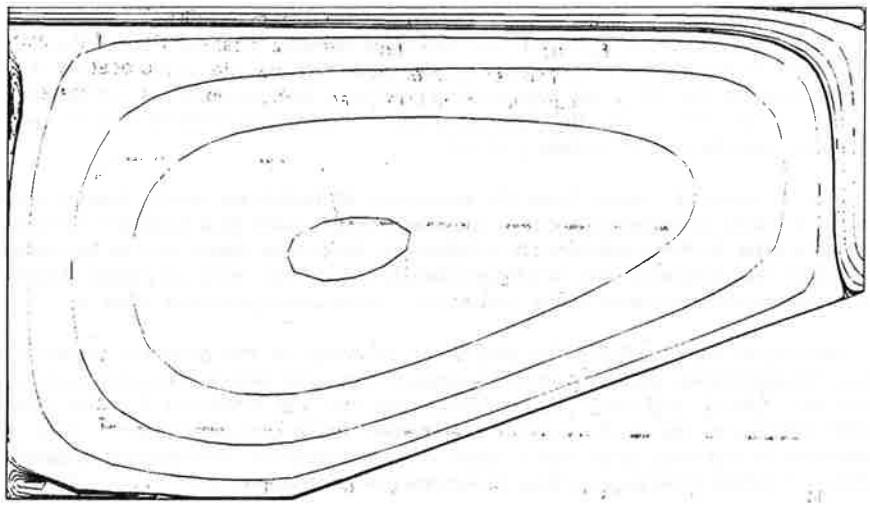

Fig.10. Streamline pattern of the flow in a geometry of the type shown in fig. 3.c. Ψ /(h.Uin) in the interval [1.3,-2.4]

The other application is the case of an enclosure with a sloping floor, of the type adopted in conference halls, and is sketched in figure 3.c. The relevant scales are h/H=0.056, L/H=3 and t/h=0.16, as in the previous two cases, and L1/H=1.

A grid with 50x50 nodes was again employed, and the Reynolds number was once more fixed at 10000. The calculated streamline pattern is shown in figure 10.

Relevant comments to the results shown are presented in the following section.

DISCUSSION

The calculations that have been described give an account of recent developments in numerical procedures that have increased the power of prediction methods in the context of room ventilation. The developments reported here cover two main areas: the calculation of low Reynolds number flow near solid boundaries, as an alternative to the adoption of turbulent wall functions, and the use of boundary fitted, non-orthogonal coordinate systems, to cope with room geometries that are not rectangular in shape.

The calculation of the near wall regions is known to require a substantial increase in grid detail to describe the steep gradients of turbulence kinetic energy and dissipation that occur in the transition layers. As shown in the profiles of figure 5, grids of the order of 50x50 nodes are too coarse to reproduce them accurately, and even the results with the finest grid tested (101x101 nodes) are still likely to contain a significant amount of grid dependence.

However, the distributions of streamlines calculated for the rectangular geometry exhibit the correct overall recirculation pattern, and the comparison of present velocity profiles with those reported in reference [2], obtained with turbulent wall functions, indicates reasonable agreement, as shown in figure 6.

In any case, the direct calculation of low Reynolds number flow becomes necessary if small details of the near wall flow must be captured, because the use of turbulent wall functions imposes that the nodes adjacent to a solid wall must be placed in the logarithmic layer, say at y^+ of at least 30. With fine grids, that minimum distance may be several times larger than the size of a typical grid cell.

Moreover, in many ventilation flows the production of turbulence kinetic energy occurs mainly in a restricted region adjacent to the inlet jets and leads to a moderate turbulence Reynolds number in the overall flow. As a result, the layers that would have to be replaced by standard wall functions tend to be considerably thick. That limitation would probably have prevented the calculation of the corner recirculation areas shown in figure 4.

Two geometries were subsequently adopted to demonstrate the ability to handle non-orthogonal boundaries., and both are extensions of the same basic rectangular shape with $h/H=0.056$, $L/H=3$ and $t/h=0.16$. In both cases the grid employed is rather coarse (50x50 nodes) and the results cannot be expected to be grid-independent. Also, the distributions of grid lines, as shown in figure 7, are simple linear distortions of rectangular meshes and exhibit unnecessarily large deviations from orthogonality.

As a result, the calculated sreamlines are not intended to present accurate quantitative information. Nevertheless, the results shown in figures 8, 9 and 10 indicate that, even in simple non-orthogonal geometries, the procedure has been able to capture a variety of flow patterns that are not accessible to methods based on cartesian coordinates.

The application to more elaborate two-dimensional geometries would not require any further modification of the procedure, and its extension to three dimensions is straightforward. However, it is recognized that the rate of convergence deteriorates as the number of grid nodes increases, This limitation is not inherent to the use of non-orthogonal grids, but indicates that the development of more efficient methods to solve the algebraic equations is in need.

CONCLUSIONS

The report described the development and application of a numerical procedure to the prediction of flows in ventilated rooms. The following summary conclusions may now be extracted:

-Using as reference for comparison published results of calculations done on a simple rectangular geometry, it has been shown that the present procedure is capable of providing an overall description of turbulent flows in ventilated rooms, with the same degree of accuracy, as results from the use of turbulent wall functions. However, a considerable amount of grid nodes must be used in the near wall layers.

-In addition, the modelling and direct calculation of the near wall layers results in better resolution of details that are beyond the reach of procedures based on the use of wall functions.

-Further results obtained in non-rectangular geometries, in spite of being associated with relatively coarse grids that limit their accuracy, indicate the ability to handle a variety of non-orthogonal geometries and produce information that is relevant in the context of room ventilation.

ACNOWLEDGEMENTS

One of the authors (F. A. Castro) has been supported by a postgraduate research grant provided by Junta Nacional de Investigação Cientffica e Tecnológica while carrying out the present study.

REFERENCES

[1]-Patankar, S. V., 1980, Numerical Heat Transfer and Fluid Flow. Hemisphere Publishing,Washington, D.C.

[2]-Nielsen, P. V., Restivo, A. and Whitelaw, J. H., 1978, The Velocity Characteristics of Ventilated Rooms. ASME J. Fluids Engineering, 100, pp. 291-298.

[3]-Thompson, J. F., Warsi, Z. U. A. and Mastin, C. W., 1985, Numerical Grid Generation:Foundations and Applications. North-Holland.

[4]-Warsi, Z. U. A. and Tiarn, W. N., 1986, Surface Mesh Generation Using Elliptic Equations. In Numerical Grid Generation in Computational Fluid Dynamics, Eds. Hauser, J. and Taylor, C., pp. 95-110.

[5]-Rhie, C. M. and Chow, W. L., 1983, Numerical Study of the Turbulent Flow Past an Airfoil with Trailing Edge Separation. AIAA J., 21, pp. 1525-1532.

[6]-Miller, T. F. and Schmidt, F. W., 1988, Use of a Pressure-Weighted Interpolation Method for the Solution of the Incompressible Navier-Stokes Equations on a Non-Staggered Grid System. Numerical Heat Transfer, 14, pp. 213, 233.

[7]-Majumdar, M., 1988, Role of Underrelaxation in Momentum Interpolation for Calculation of Flow with Non-Staggered Grids. Numerical Heat Transfer, 13, pp. 125, 132.

[8]-Jones, W. P. and Launder, B. E., 1973, Predictions of Low Reynolds Number Phenomena with a Two-Equation Model of Turbulence. Int. J. Heat and Mass Transfer, 16, pp.1119-1130.

[9]-Lam, C. K. G. and Bremhorst, K. A., 1981, Modified Form of the K-e Model for Predicting Wall Turbulence. ASME J. Fluids Engineering, 103, pp. 456-460.